Quantitative image analysis of microplastics in bottled water using Artificial Intelligence

Clementina Vitali[1,2]*, Ruud J. B. Peters[1], Hans-Gerd Janssen[2,3], Anna K. Undas[1], Sandra Munniks[1], Francesco Simone Ruggeri[2,4]* , Michel W. F. Nielen[1,2]

[1] Wageningen Food Safety Research, Wageningen University & Research, Akkermaalsbos 2, 6708 WB Wageningen, The Netherlands.

[2] Wageningen University, Laboratory of Organic Chemistry, Stippeneng 4, 6708 WE, Wageningen, The Netherlands.

[3] Unilever Foods Innovation Centre – Hive, Bronland 14, 6708 WH Wageningen, The Netherlands.

[4] Wageningen University, Physical Chemistry and Soft Matter, Stippeneng 4, 6708 WE, Wageningen, The Netherlands.

* Corresponding authors:

Email: clementina.vitali@wur.nl

simone.ruggeri@wur.nl

Abstract

The ubiquitous occurrence of microplastics (MPs) in the environment and the use of plastics in packaging materials result in the presence of MPs in the food chain and exposure of consumers. Yet, no fully validated analytical method is available for microplastic (MP) quantification, thereby preventing the reliable estimation of the level of exposure and, ultimately, the assessment of the food safety risks associated with MP contamination. In this study, a novel approach is presented that exploits interactive artificial intelligence tools to enable automation of MP analysis. An integrated method for the analysis of MPs in bottled water based on Nile Red staining and fluorescent microscopy was developed and validated, featuring a partial interrogation of the filter and a fully automated image processing workflow based on a Random Forest classifier, thereby boosting the analysis speed. The image analysis provided particle count, size and size distribution of the MPs. From these data, a rough estimation of the mass of the individual MPs, and consequently of the MP mass concentration in the sample, could be obtained as well. Critical materials, method performance characteristics, and final applicability were studied in detail. The method showed to be highly sensitive in sizing MPs down to 10 µm, with a particle count limit of detection and quantification of 28 and 85 items/500 mL, respectively. Linearity of mass concentration determined between 10 ppb and 1.5 ppm showed a regression coefficient of (R^2) of 0.99. Method precision was demonstrated by a repeatability of 9 - 16% RSD (n = 7) and within-laboratory reproducibility of 15 - 27 % RSD (n = 21). Accuracy based on recovery was 92 ± 15 % and 98 ± 23 % at a level of 0.1 and 1.0 ppm, respectively. The quantitative performance characteristics thus obtained complied with regulatory requirements. Finally, the method was successfully applied to the analysis of twenty commercial samples of bottled water, with and without gas and flavor additives, yielding results ranging from values below the limit of detection to 7237 (95% CI [6456, 8088]) items/500 mL.

Keywords

Microplastic; bottled water; artificial intelligence; Nile Red; fluorescence microscopy; method validation.

Abbreviations

AI, artificial intelligence; AOAC, Association of Official Analytical Chemists; CI, confidence interval; csv, comma separated values; DL, detection limit; H5, Hierarchical Data Format version 5; IQR, interquartile range; LDPE, low-density polyethylene; LOQ, limit of quantification; mLOD, method limit of detection; MP, microplastic; MPs, microplastics; ND, not detected; PA 6, polyamide-6; PE, polyethylene; PET, poly(ethylene terephthalate); PMMA, poly(methyl methacrylate); PS, polystyrene; PTFE, poly(tetrafluoro ethylene); PVDC, and poly(vinyl denechloride); RSD, relative standard deviation; SI, supplementary information; SD, standard deviation; SDS, sodium dodecyl sulfate; tif, tagged image file format.

Introduction

The extensive use of plastics and the wide spread occurrence of plastic debris in the environment have resulted in the presence of microplastics (MPs), defined as plastic particles whose longest distance measures from 1 µm to 5000 µm [1]. MPs occur in most ecosystems including oceans [2], freshwaters [3], and agricultural soil [4]. Consequently, the presence of MPs along the food chain has been reported [5], drawing attention to the possible exposure of consumers [6–8].

As it has not been clarified yet whether MPs may potentially represent a threat to human health, the understanding of the abundance and properties of this emerging contaminant has become a key societal and scientific challenge. However, no fully validated analytical method is available for the quantification of MPs [9] and the data available in the literature are insufficient for a reliable estimation of microplastic (MP) exposure, hence for assessing the food safety risk related to MP contamination [5]. For the analysis of contaminants in the agri-food chain, the method *fit-for-purposeness* is usually assessed by comparing performance characteristics with regulatory requirements or defined target values. The lack of official guidelines and standard reference material is partially accountable for the unavailability of validated methods for the analysis of MPs. As a matter of fact, it has not even been determined yet whether the quality parameters conventionally used for analytical method validation are suitable for the evaluation of imaging-based MP quantification methods, that are the most widespread practice in MP analysis.

The analysis of bottled water represents a convenient starting point for analytical development and method validation. Several analytical techniques have been applied to the analysis of MPs in bottled water, including optical [10–13] and fluorescence [12,14] microscopy, atmospheric solids analysis probe mass spectrometry [15], (micro-)Fourier-transform infrared spectroscopy [11,12,14,16], (micro-)Raman spectroscopy [11,13,14,17,18] and scanning electron microscopy [13,16] with energy dispersive X-ray analysis [19,20]. Among these, Nile Red staining coupled with fluorescence microscopy [12,14]

standsout as a simple and affordable approach, ideal to be evaluated for its suitability to obtain a quantitative analysis of MPs. Nile Red is a solvatochromic dye with intense fluorescence when sequestrated in a hydrophobic pocket. It has successfully been applied to the selective staining of plastic particles [21–30], occasionally in combination with semi-automated image processing for particles characterization [31–34]. The analysis of MPs following Nile Red staining does not require the use of specialized and expensive instruments and can be, in theory, performed by non-specialized personnel. Despite the potential of this strategy, a complete, time efficient, reliable, and robust method integrating sample preparation, image acquisition, and fully automated image- and data processing has not been described yet.

Semi-automated image processing for the analysis of Nile Red stained MPs involves the segmentation of the fluorescence image into a background and a foreground and the production of binarized masks that can be further processed by object counting algorithms. The image segmentation relies on the selection of an intensity threshold. The manual selection of threshold values [33,34] or the use of algorithms for automated threshold selection [35] are both reported as suitable options but have, so far, yielded methods described as insufficiently robust [33,35]. The lack in robustness results in the production of variable results and prevents the evaluation of the quantitative and qualitative performance characteristics of the method. Consequently, the automation of MP analysis remains a significant challenge.

In recent years, advancements in technology have opened up new avenues for analytical chemists to explore, particularly in the realm of artificial intelligence (AI). Traditional machine learning algorithms in combination with advanced statistical methods have long been used to process complex data sets, but often required extensive coding skills [36]. With the availability of interactive tools analytical chemists now have facilitated accessibility to AI, which can be applied at different stages of the research process, even without programming proficiency.

This study aims to contribute to the automation of MP analysis by presenting a novel approach that exploits interactive AI tools to address some of the challenges arising in the development and validation of methods for the analysis of MPs. Here, we present an integrated method for the quantitative analysis of MPs in bottled water based on Nile Red staining, fluorescence microscopy, and automated image processing (**Figure 1**). A supervised machine learning tool (Ilastik [37]) was used to develop a Random Forest classifier for the semantic segmentation of fluorescence images of Nile Red stained MPs, resulting in a sensitive, specific, and robust detection workflow able to overcome the limitations of previous threshold selection approaches. The performance of the method was validated against common analytical criteria such as limit of detection and limit of quantification, linearity and linearity range, repeatability, within-laboratory reproducibility and recovery, and its applicability was tested by the analysis of 20 samples of commercial bottled water containing a range of different flavoring and additives.

Materials and methods

Reagents and standards. Polyethylene MPs (ultra-high molecular weight, surface-modified, polyethylene powder, 40-48 µm, Sigma-Aldrich, Schnelldorf, Germany) (PE) were spiked in ultrapure water and used in both method development and performance assessment. The accuracy of particle size measurements was assessed using polystyrene (PS) analytical standards from Sigma-Aldrich with certified particle sizes and standard deviations (5 ± 0.16 µm, 10 ± 0.11 µm, 30 ± 0.29 µm, 100 ± 1.6 µm, 150 ± 1.8 µm, 200 ± 2.3 µm). The staining protocol was also tested on low-density polyethylene (LDPE) 300 µm, polyamide-6 (PA 6) 55 µm, poly(hydroxy butyrate) / poly(hydroxy valerate) 2% biopolymer 300 µm, poly(ethylene terephthalate) (PET) 300 µm, poly(tetrafluoro ethylene) (PTFE) 20 µm, and poly(vinyl denechloride) (PVDC) <180 µm, all from Goodfellow (Hamburg, Germany); blue PE microsphere 125 – 150 µm was purchased from Cospheric (Santa Barbara, California); and, microparticles based on poly(methyl methacrylate) (PMMA) 100 µm were purchased from Sigma-Aldrich. Aqueous MPs

suspensions were prepared in 0.02% Tween20 (Sigma Aldrich), 0.02% sodium dodecyl sulfate (SDS), (Sigma Aldrich), or 0.02% Triton X-100 (Merk, Darmstadt, Germany). A stock solution of Nile Red (Sigma-Aldrich) was prepared in HPLC-grade acetone (Actu-All Chemicals, Oss, Netherlands) and diluted in HPLC-grade ethanol (Supelco, Darmstadt, Germany). Ultrapure water was obtained in-house from a MilliQ Water Purification System (Merk) and tested for the absence of MPs as described in the contamination prevention section.

Samples. The applicability of the method was tested on 20 bottled water samples purchased at a local store. Details on the sales denomination, water origin, bottle material, and volume are available in the supplementary information (Table S1).

Filtration. Filtration was performed using a glass vacuum filtration device (Sartorius) connected to a mini diaphragm vacuum pump (model VP 86, VWR, Amsterdam, Netherlands). Several filters were tested for their compatibility with the method: black polycarbonate membrane filters (pore size 0.2 µm, diameter 25 mm. Whatman, Maidstone, United Kingdom), alumina-based filter membranes (Anodisc, pore size 0.2 µm, diameter 25 mm, Whatman), cellulose nitrate filters (pore size 0.2 µm, diameter 25 mm, Whatman).

Contamination prevention. To prevent environmental contamination of samples and standards, the following good practices were incorporated into the method and considered mandatory preparatory steps prior to sample preparation: (I) lab work on samples took place only under laminar bench flow; (II) 100% cotton lab coats were worn during operations; (III) only 100% non-particle releasing nitrile gloves were worn during the operations; (IV) any piece of glassware used during the operations was washed, additionally to the routine cleaning procedure, with ultrapure water and a suitable surfactant and rinsed in analytical grade acetone prior to use; (V) samples were always covered with aluminium foil or clean glassware; (VI) metallic labware was rinsed with analytical grade acetone prior to use.

Verification of adequate contamination prevention measures was performed by analysing blank samples of ultrapure water.

Development of Nile Red staining procedure. The staining procedure was adapted from the study by Konde *et al.*. [24]. Briefly, a 0.5 mg/mL stock solution of Nile Red in acetone was prepared and further diluted in ethanol to obtain a 20 µg/mL staining solution. An adequate volume of staining solution was added to each sample to a final level of 0.4 µg/mL. Samples were incubated for 15 minutes and filtered. Then, each filter was laid on a glass microscope slide and protected with a coverslip tightly taped onto the microscope slide. The staining protocol was tested on a set of different polymers, namely PE, LDPE, PS, PA 6, PET, PTFE, PVDC, and PMMA. Three different surfactants were tested to obtain a homogeneous dispersion of MPs in the water matrix: SDS, Triton X-100, and Tween20. 4 mg of PE were dispersed in 100 mL of a 0.2% solution of each surfactant in ultrapure water. After staining, three aliquots of 25 mL were sampled, filtered, and analyzed via fluorescence microscopy and automated image analysis according to the protocol developed and evaluated in this study. Similarly, different filter materials were tested for their suitability for the fluorescence detection of Nile Red stained MPs. All filters had a diameter of 25 mm and a pore size of 0.2 µm. 0.1 ppm and 1 ppm suspensions of PE in ultrapure water with 0.2% Tween20 were stained; three aliquots of the MP suspension were filtrated using black polycarbonate, alumina, and cellulose nitrate membrane filters. Stained particles on the filters were analyzed via fluorescence microscopy and automated image analysis according to the ImageJ-based protocol developed and evaluated in this study.

Image data acquisition. Images were acquired with an Olympus BX51 microscope, equipped with Olympus 4x, 10x, 20x and 40x objectives, an Olympus SC50 RGB camera, an Olympus U-RFL-T UV lamp, and a bandpass filter characterized by excitation and emission wavelengths of, respectively, 460-490 nm and > 515 nm. The images, acquired by cellSens software (Olympus), were saved in Tagged Image File Format (.tif). Twenty-one images (1.4 mm x 1.1 mm) were taken for each filter. To keep into account the

inhomogeneous distribution of the particles, the surface of the filter was divided into three concentric regions of equal areas (an inner disk encircled by a mid and an outer annuli), and the same number of pictures was taken for each region. A schematic diagram for the image data acquisition is given in the supplementary information (Figure S1).

Image data processing. Image processing was performed on a PC HP Core (TM) i5-9400 CPU @ 2.90GHz (16.00 GB RAM) with a Windows 10 64-bit operating system.

Initially, a workflow for image processing was developed entirely in ImageJ (https://imagej.nih.gov/) including an automated algorithm for threshold selection and segmentation of fluorescence images of Nile Red stained MPs. This workflow was meant for later comparison with the novel Random Forest classifier approach hereby proposed. We will further refer to the workflow entirely developed in ImageJ as "ImageJ-based workflow"; while we will refer to the workflow that includes the Random Forest classifier as "Ilastik-based workflow". Briefly, in the ImageJ-based workflow, the macro splits each image into three color channels and selects the green channel for further processing. An automated threshold (labeled "Li" in ImageJ after the author who developed the iterative algorithm for minimum cross entropy thresholding [38] integrated into the software) is then used to binarize the image., Overlapping particles are distinguished by applying the watershed function, and the noise is reduced by replacing pixels that deviate from the median of their surrounding in a radius of 10 pixels (a function labelled "remove outliers" in ImageJ). Once the pre-processing is completed, particle count and particle sizes are measured by the "analyze particle" function. In addition, the MPs mass is calculated: first the particle volume is roughly estimated by assuming that the individual particle shapes are ellipsoidal and that the third dimension of the MP equals the minor axis of the best-fitting ellipse, as previously reported [4,39]. Finally, using polymer density data, the MP mass is estimated and registered in the comma-separated value (csv) file generated by ImageJ for each image. The cumulative weight of all particles detected in each image is calculated and registered as well. Such an MP mass estimation

procedure based on 2D data and 3D shape assumption is considered, so far, the best approach to handle MPs data as mass concentration instead of particle count [39–41]. The thresholding algorithm developed by Li *et al*. [38] works by minimizing the cross-entropy between the foreground and the foreground mean and the background and the background mean, therefore it is dependent on the presence of at least one particle per image. In the case of pictures not containing fluorescent particles, the background noise interferes with the threshold calculation and yields false positive results. In an attempt to overcome this important issue, our macro artificially adds a particle (Figure S2) to the top left corner of each picture. This particle is always reported in the first row of the csv file and ignored in the subsequent calculation of cumulative weight and in the data analysis.

A second workflow for image processing was then developed, introducing for the first time in the field of MP analysis the use of Ilastik (https://www.ilastik.org/ [37]) to train a supervised machine learning algorithm for the semantic segmentation of fluorescence images of Nile Red stained MPs - or, in other words, to replace the automated threshold selection algorithm. The Random Forest classifier was trained on a set of 55 images, including images of blank ultrapure water samples, real samples, and PE, PA6, PET, and PVDC Nile Red stained MPs. Before proceeding with the evaluation of the method performance, the classifier was tested on a test set including images of standard MPs at different concentrations, blank ultrapure water samples, and real samples (**Figure 2**). The model was further trained until the production of binarized masks resulted satisfactory. It is worth noting that none of the images used in the training set was included in the test set or in the assessment of method performance and applicability. Also, in the Ilastik-based workflow, a first macro in ImageJ artificially adds a particle (Figure S2) to the top left corner of each picture and converts the images in the Hierarchical Data Format version 5 (H5). The headless mode of the Ilastik platform is then used to process the images in batches and to produce binarized masks. A second ImageJ macro applies the watershed function, the remove outliers function, and analyzes the particles as described above. In the Ilastik-based workflow, the

addition of a particle in each image is made necessary by the object counting algorithm included in ImageJ, which is designed to produce an error when no automatic threshold is set for image segmentation and no particle is detected – here no automated threshold selection algorithm is set in ImageJ because the software is provided with binary images that were previously segmented in Ilastik.

Data analysis. After image processing, the analysis is completed by computing the total particle number or the total weight of MPs on the filter. To this end, a script in R was developed to elaborate the information contained in the 21 csv files generated for each sample. In addition, the confidence interval (CI) of the analysis is computed by bootstrapping. Statical analysis was performed in RStudio (Windows Version 1.3.959) and Excel Office360 (Microsoft, San Francisco, CA, USA).

Method performance assessment. As no guidelines nor dedicated legislation is available for MP analysis, general criteria derived from the Association of Official Analytical Chemists (AOAC) Guidelines for Single Laboratory Validation of Chemical Methods for Dietary Supplements and Botanicals [42] were used to set target values for quantitative performance assessment of the developed method. These guidelines were outlined based on common method validation practice for chemical analysis, where methods are evaluated for their reliability in quantitating analytes as molecules in solutions of known concentration. In the peculiar case of MPs, we aim at counting the number of particles in suspension. However, the preparation of suspensions containing a known and accurate number of MPs is still an unresolved issue. Therefore, to partially overcome this problem and to best align with the above-mentioned guidelines, we evaluated the performance of our method based on the computed weight of the stained particles against the weight of PE powder as measured by an analytical balance with a readability of 0.1 mg. This strategy implies the assumption that a method able to quantitate the mass concentration of plastic particles dispersed in the spiked samples with a certain degree of reliability is equally reliable in yielding results expressed as number of particles.

The accuracy of particle sizing was estimated by measuring Nile Red stained PS analytical standards with certified particle sizes ranging from 5 to 200 µm, linearity within this working range was also verified.

The method limit of detection (mLOD) in terms of particle number was estimated based on seven blank samples (ultrapure water) as the mean number of particles plus 3 times the standard deviation. The limit of quantification (LOQ) was calculated as 3 times the mLOD.

Linearity within the working range of 0.01 – 1.5 ppm was studied by the analysis of PE spiked ultrapure water. Similarly, the repeatability as relative standard deviation (RSD, %) was determined from the analysis of seven samples of ultrapure water spiked at a level of 0.10 ppm and 1.00 ppm. The reproducibility (here, the within-laboratory reproducibility) was estimated from the analysis of seven ultrapure water samples spiked at a level of 0.10 ppm and 1.00 ppm, the experiments were repeated on 3 different days. The computed recovery from the image data analysis was evaluated on ultrapure water samples spiked at a level 0.10 ppm and 1.00 ppm.

Analysis of microplastics in bottled water. An adequate volume of Tween20 was added to each sample to a final 0.2% concentration (v/v). 500 mL of each water sample were filtrated on a black polycarbonate membrane filter. After filtering 475,5 mL of sample, the filtration was put on hold, the remaining 24.5 mL were poured into the filtration unit, 500 µL of staining solution were added, and the solution was incubated for 15 min. Afterwards, the filtration was completed, and the filter was stored as previously described.

Interactive artificial intelligence tools. Three interactive AI tools were used in this work at different stages of the research process. Firstly, Ilastik (https://www.ilastik.org/) was used to train a supervised machine learning algorithm for the semantic segmentation of fluorescence images of Nile Red stained MPs, as described above. Then ChatGPT (https://chat.openai.com/chat) was used to polish the scripts and macros developed in this study for automated image analysis. ChatGPT is a large language model

based on the GPT-3.5 architecture that uses deep learning techniques to generate human-like responses to natural language inputs. In particular, a prompt was provided to ChatGPT to improve the readability and efficiency of the scripts. Lastly, DALL-E (https://labs.openai.com/) was used to generate the graphical abstract for this publication. DALL-E is an artificial intelligence model that can generate images from textual descriptions using deep learning techniques. The prompts provided to DALL-E were “a female scientist holding a water bottle”, “a neon cyborg staring at a galaxy inside a microscope”, “a laptop with a forest as wallpaper”, “a stack of paper”, “a hand holding a paper sheet” to represent the development of the staining procedure, the use of fluorescence microscopy to acquire the images of Nile Red stained MPs, the use of a Random Forest classifier for image processing, the huge quantity of data automatically processed by our method, and the generated results, respectively. Particle count and particle size distribution illustrated in the paper sheet were added manually.

Results and discussion

The objective of developing this method for the analysis of MPs based on Nile Red staining, fluorescence microscopy, and automated image processing was to deliver a reliable, fast, and easy protocol for the quantification of MPs in drinking water. Critical conditions, data processing and applicability to real samples were studied in more detail.

Critical reagents and materials used for sample preparation. Staining conditions as optimized by Konde *et al.* [24] showed to be successful in the staining of our rather heterogenous set of MPs. However, the addition of a surfactant was crucial to prevent MPs from agglomerating or adhering to the walls of the glassware and to yield satisfactory recovery values. No statistical significance was observed in the recovery of PE MPs dispersed in ultrapure water upon using either SDS, Triton X-100, or Tween20 (one-way ANOVA test, $p = 0.75$). Tween20 was selected for further experiments in an effort to minimize contamination: it was available in glass packaging. Then, we evaluated the compatibility of different

filters with fluorescence microscopy and imaging analysis and their effect on the ability to quantify MPs. **Figure 3** illustrates Nile Red stained PE particles isolated on different filters and shows the results of a recovery study performed on these filters. By comparing the computed recovery values obtained on polycarbonate, alumina, and cellulose nitrate membrane filters, we observed that the filter material significantly affects particle quantification (one-way ANOVA test, $p = 2.3*10^{-7}$ at a concentration of 0.1 ppm and $p = 2.2*10^{-4}$ at a concentration of 1 ppm). Alumina-based and cellulose nitrate filters (**Figure 3B-C**) showed a more intense background fluorescence that interfered with the image segmentation and resulted in computed recovery values higher than 200%. A Student t-test was performed to compare polycarbonate and alumina-based filters, the different performance ($p = 2*10^{-3}$ and $p = 3.4*10^{-2}$ at 0.1 ppm and 1 ppm, respectively) might be explained by the more tricky handling of alumina filters: MPs isolated on their surface are easily displaced. This results in particle agglomerates that interfere with the correct image segmentation, object classification, and ultimately quantification. The use of polycarbonate filters yielded the best computed recovery values at both 0.1 and 1 ppm levels (**Figure 3D**).

Image data processing. Both the ImageJ-based- and the Ilastik-based workflows were tested against common performance evaluation criteria such as limit of detection and limit of quantification, linearity and linearity range, repeatability, within-laboratory reproducibility, and recovery, and their applicability was tested by the analysis of real samples of bottled water. The evaluation of method performance was positive for both the ImageJ-and the Ilastik-based workflows, however, the ImageJ-based workflow presented major flaws in terms of robustness. Despite being able of correctly sizing and quantifying Nile Red stained standard PE (Table S2), the ImageJ-based workflow was unable to perform a satisfactory fragmentation of images acquired from the analysis of blank and real samples. Consequently, portions of the background were included in the calculation of the mLOD and LOQ. This, in addition to the inability of the segmentation algorithm to properly binarize most of the images acquired for the real sample

analysis, caused the failure of the ImageJ-based workflow in the applicability performance test. In contrast, the Ilastik-based workflow was trained to perform successful segmentation also on blank ultra-pure water samples and real sample of bottled water, overcoming the robustness issues related to the use of the automatic calculated threshold and improving the mLOD and LOQ. The scripts as developed and optimized in this study are available as GitHut repository (https://doi.org/10.5281/zenodo.7809431). The results of the performance evaluation of the Ilastik-based workflow are further detailed and discussed below.

Automation potential of the protocol. Sample preparation - including contamination prevention, staining, incubation, filtration, and slide preparation for microscopic analysis – can be considered as the time-limiting step in the proposed protocol. However, multiple samples can be processed in parallel. Thus, despite the extra care necessary for contamination prevention and in handling the filters to prevent particle loss or displacement, the protocol can be routinely performed by non-expert – but obviously trained – personnel. Following the automated image acquisition of a subsample of the whole membrane filter - whose duration depends on the autofocus performance of the camera and on exposure times - the fully automated image and data analysis, featuring the Ilastik-based workflow, allow the effortless completion of the analysis within 15 to 20 min per sample or replicate.

Performance characteristics of the Ilastik-based workflow. The method mLOD in terms of particle count is 28 items/500 mL, calculated as the mean number of fluorescent particles in 7 blank samples plus 3 times the standard deviation. The LOQ is 85 items/500 mL, calculated as 3 times the mLOD.

While the resolution of microscopy techniques depends on the underlying physics and is well established, the performance of algorithms for the automatized image segmentation can affect size measurements and the estimation of particle weight thereof [43]. Therefore, the accuracy in particle size measurement was assessed by the analysis of analytical standards of PS microspheres with certified

diameter. **Figure 4A** shows the average measured diameter as a function of the nominal diameter of 10, 30, 100, 150, and 200 µm microspheres. As expected, the data are on a straight line with a unitary angular coefficient. As the accuracy in measuring 5 µm Nile Red stained PS microsphere failed (relative error of 111%, n = 5), 10 µm was set as the lower detection limit of the method. Accordingly, only fluorescent particles with a major dimension larger than 10 µm were included in the quantitative image data analysis.

The working range in mass concentration spans from 1.1 ppb to 1.5 ppm (**Figure 4B**). Linearity was studied in the concentration range of 0.01 – 1.5 ppm and resulted in a very good regression coefficient of R^2 = 0.99 (target value 0.98-0.999 [42]). The repeatability of mass concentration, determined from the analysis of 7 spiked ultrapure water samples (**Figure 4C**), is 16% RSD (relative standard deviation) at the concentration of 0.10 ppm and 9% RSD at 1.00 ppm (target values ranging from 5.5 to 22% and from 4 to 16% [42], respectively). The within-laboratory reproducibility, determined from the analysis of 7 spiked ultrapure water samples on 3 different days (**Figure 4C**), is 27% RSD at 0.10 ppm and 15% RSD at 1.00 ppm (target values ranging 11.5 – 46 % and 8 – 32 % for 0.1 ppm and 1.0 ppm [42], respectively).

As no reference material is available, a recovery study was performed to estimate the trueness of the method (**Figure 4D**). The computed recovery of MPs spiked in ultra-pure water is 89 ± 23 % (mean ± SD, n = 21) at a concentration of 0.1 ppm and 92 ± 15 % (mean ± SD, n = 21) at 1.0 ppm. The recovery complies with the target values of 70-120 % and 75-120 % at 0.1 and 1 ppm [42], respectively.

Since the analyses are performed only on a sub-section of the whole membrane filter, the quantitative result of each analysis should be provided with an expanded measurement uncertainty that is an interval for the result of a measurement expected to contain a large part of the distribution of values that can result from the measurement. Accordingly, a bootstrap estimation was performed, and the 95% CI is reported.

The results of the quantitative performance evaluation not only proof the suitability of this method for the analysis of MPs in bottled water, but also demonstrate that conventional performance parameters used in regulatory frameworks, can also be applied to the field of MP analysis.

Applicability to microplastics analysis in bottled water samples. Twenty samples of bottled water purchased at a local Dutch store were analyzed for MP contamination. The sample set was quite heterogeneous and comprised still, sparkling, carbonated, mineral, spring, filtered, and flavored waters and combinations thereof, for details see Table S1. Additives and ingredients were not found to intherfere with the method. The 70% of the analyzed samples of bottled water showed Nile Red stained particle numbers higher than the LOQ; only one real sample turned out to be blank. **Figure 5A** illustrates the quantification of fluorescent particles in the samples that show a contamination level above the limit of detection. A boxplot chart was used to visualize the bootstrap estimate and the 95% CI of each quantitative measurement, the data used to build the chart are available in the SI (Table S3). The contamination level in still waters ranges from values below the LOQ to a maximum of 972 (95% CI [625, 1372]) items in 500 mL; in sparkling waters to a maximum of 1007 (95% CI [521, 1579]) items in 500 mL. In flavored waters, the MP count ranges from values below the mLOD up to 7237 (95% CI [6456, 8088]) items in 500 mL. **Table 1** reports the occurrence of MPs in bottled water as found in previous studies. Overall, our results are in the same order of magnitude as data previously reported in Germany [17] and Iran [44]. Lower levels of MP contamination were observed in most of the previous studies [10,11,16,18,19,45–52]; while two studies reported considerably higher particle count data [53,54]. Quantitative data regarding the occurrence of MPs in bottled water spans by several orders of magnitude not only from study to study but also from sample to sample within the same study [12,44]. A more widespread use of analytical methods that feature validated performance characteristics would enable a more thorough comparison among literature data and would allow to discuss the variability observed within and between individual datasets. Preliminary studies have suggested few hypotheses to

explain this valiability, including the effect of water bottle storing conditions and duration [44], the rheologic property of the polymers used for the production of the bottles [55], and the handling of the bottles [19].

With respect to particle size in the real samples, the major dimension of the analyzed particles was evaluated. The 96% of the analyzed particles measured less than 50 µm, while only 1% of the particles was larger than 100 µm. The size of the smallest detected particles overlaps with the detection limit of 10 µm, and the largest detected particle measures 310 µm. The size distributions of the fluorescent particles isolated from each sample are reported in **Figure 5B**, and the data used to build the chart are included in SI (Table S4). The medians range from 14 to 35 µm, and all distributions are right-skewed, coherently with the substantial portion of the analyzed particles measuring less than 20 µm (69%). The particle size distribution of our dataset is consistent with previous literature in reporting that particles smaller than 50 µm provide the larger contribution to MP contamination in bottled water [12,18,46,51,53]. The skewness of the particle size distributions illustrated in **Figure 5B,** in agreement with the findings of studies that report a size detection limit closer to 1 µm [18,44,53,54], highlights the importance of the development of analytical methods able to detect and characterize plastic particles down to the nanometer scale in order to get a comprehensive profile of the synthetic polymer contamination in bottled water.

[Please, insert Table 1 here]

Artificial intelligence interactive tools. To further contribute to the automation of MP analysis, interactive AI tools were used to address some of the challenges arising in the method development. The use of Ilastik for the training of a supervised machine learning model yielded, as thoroughly discussed above, a robust workflow for the segmentation of fluorescence microscopy images of Nile Red stained MPs. Due to its proven reliability, the workflow minimalize operator supervision and enabled the full automation of the image processing part of the method. The application of ChatGPT for polishing

the scripts to improve their efficiency and readability slightly improved the performance of the method in terms of time, but above all enabled the authors to share more elegant and professional pieces of code, easier to understand, modify, and maintain. Lastly, the assistance of DALL-E for the generation of a graphical abstract allowed the authors to achieve in about two hours – including the time necessary to master the use of the platform – a professional and visually-striking representation of the developed method, all while being a cost-effective solution.

Conclusions

In this study, a critical evaluation of MP quantification based on Nile Red staining, fluorescence microscopy, and automated image processing was performed. A Random Forest classifier was trained to achieve a robust semantic segmentation of fluorescence images of Nile Red stained MPs, key for a reliable automated MP quantification. The accuracy of the method in sizing and quantifying MPs was assessed. Repeatability, within-laboratory reproducibility, and recovery complied with the AOAC general criteria for analytical methods. Conventional quality parameters, regularly used for the validation of analytical methods, showed to be applicable to the assessment of method performance. The method was applied to a heterogeneous range of commercial bottled water samples and their ingredients were found not to interfere with the developed method. Particle count ranged from levels below the mLOD to 7237 (95% CI [6456, 8088]) items/500 mL and particle sizes from 10 to 310 µm. The size range spanning from 10 to 20 µm mainly contributes to MP contamination in bottled water, accounting for 69 % of the analyzed particles.

A reliable, high throughput, and effortless protocol for the quantitative analysis of MPs is now available for further development in the field of MP analysis in food. Newly developed sample preparation procedures for the isolation of MPs from more complex food sample matrices can be critically assessed using the validated analysis protocol presented. It is worth noting that, even if modifying the method is

necessary to adapt the protocol to more complex samples and a new training is required, the Ilastik platform allows to do it so easily and fastly.

Electronic Supplementary data

Script and macros developed in this project are available at https://doi.org/10.5281/zenodo.7809431.

Acknowledgments

This project has received funding from the European Union's Framework Programme for Research and Innovation Horizon 2020 under the Marie Skłodowska-Curie Grant Agreement No. 860775, MONPLAS.

The authors thank Martin Alewijn for his contribution to the assessment of analytical uncertainty and providing R script implementation.

References

[1] International Organization for Standardization. Plastics — Environmental aspects — State of knowledge and methodologies (ISO/TR 21960:2020)., 2020. https://www.iso.org/standard/72300.html.

[2] R. Gillibert, G. Balakrishnan, Q. Deshoules, M. Tardivel, A. Magazzu, M.G. Donato, O.M. Marago, M. Lamy, D. La Chapelle, F. Colas, F. Lagarde, P.G. Gucciardi, Raman Tweezers for Small Microplastics and Nanoplastics Identification in Seawater, Environ. Sci. Technol. 53 (2019) 9003–9013. https://doi.org/10.1021/acs.est.9b03105.

[3] M. González-Pleiter, M. Tamayo-Belda, G. Pulido-Reyes, G. Amariei, F. Leganés, R. Rosal, F. Fernández-Piñas, Secondary nanoplastics released from a biodegradable microplastic severely impact freshwater environments, Environ. Sci. Nano. 6 (2019) 1382–1392. https://doi.org/10.1039/c8en01427b.

[4] F. Corradini, P. Meza, R. Eguiluz, F. Casado, E. Huerta-lwanga, V. Geissen, Evidence of microplastic accumulation in agricultural soils from sewage sludge disposal, Sci. Total Environ. 671 (2019) 411–420. https://doi.org/10.1016/j.scitotenv.2019.03.368.

[5] C. Vitali, R. Peters, H.-G. Janssen, M.W.F. Nielen, Microplastics and nanoplastics in food, water, and beverages; part I. Occurrence, TrAC Trends Anal. Chem. (2022). https://doi.org/10.1016/j.trac.2022.116670.

[6] K.D. Cox, G.A. Covernton, H.L. Davies, J.F. Dower, F. Juanes, S.E. Dudas, Human Consumption of Microplastics, Environ. Sci. Technol. 53 (2019) 7068–7074. https://doi.org/10.1021/acs.est.9b01517.

[7] N.H.M. Nor, M. Kooi, N.J. Diepens, A.A. Koelmans, Lifetime Accumulation of Microplastic in Children and Adults, Environ. Sci. Technol. 55 (2021) 5084–5096. https://doi.org/10.1021/acs.est.0c07384.

[8] Q. Zhang, E.G. Xu, J. Li, Q. Chen, L. Ma, E.Y. Zeng, H. Shi, A Review of Microplastics in Table Salt, Drinking Water, and Air: Direct Human Exposure, Environ. Sci. Technol. 54 (2020) 3740–3751. https://doi.org/10.1021/acs.est.9b04535.

[9] C. Vitali, R.J.B. Peters, H.-G. Janssen, M.W.F. Nielen, F.S. Ruggeri, Microplastics and nanoplastics in food, water, and beverages, part II. Methods, Trends Anal. Chem. 157 (2022) 116819. https://doi.org/10.2139/ssrn.4061397.

[10] M. Kosuth, S.A. Mason, E. V. Wattenberg, Anthropogenic contamination of tap water, beer, and sea salt, PLoS One. 13 (2018) 1–18. https://doi.org/10.1371/journal.pone.0194970.

[11] P. Makhdoumi, A. Ahmad, H. Karimi, M. Pirsaheb, H. Kim, H. Hossini, Occurrence of microplastic particles in the most popular Iranian bottled mineral water brands and an assessment of human exposure, J. Water Process Eng. 39 (2021) 101708. https://doi.org/10.1016/j.jwpe.2020.101708.

[12] S.A. Mason, V.G. Welch, J. Neratko, Synthetic Polymer Contamination in Bottled Water, Front. Chem. 6 (2018) 407. https://doi.org/10.3389/fchem.2018.00407.

[13] V.C. Shruti, F. Pérez-Guevara, I. Elizalde-Martínez, G. Kutralam-Muniasamy, First study of its kind on the microplastic contamination of soft drinks, cold tea and energy drinks - Future research and environmental considerations, Sci. Total Environ. 726 (2020) 138580. https://doi.org/10.1016/j.scitotenv.2020.138580.

[14] D. Kankanige, S. Babel, Smaller-sized micro-plastics (MPs) contamination in single-use PET-bottled water in Thailand, Sci. Total Environ. 717 (2020) 137232. https://doi.org/10.1016/j.scitotenv.2020.137232.

[15] C. Vitali, H.G. Janssen, F.S. Ruggeri, M.W.F. Nielen, Rapid Single Particle Atmospheric Solids Analysis Probe-Mass Spectrometry for Multimodal Analysis of Microplastics, Anal. Chem. 95 (2023) 1395–1401. https://doi.org/10.1021/acs.analchem.2c04345.

[16] X. Zhou, J. Wang, H. Li, H. Zhang, Hua-Jiang, D.L. Zhang, Microplastic pollution of bottled water in China, J. Water Process Eng. 40 (2021) 101884. https://doi.org/10.1016/j.jwpe.2020.101884.

[17] B.E. Oßmann, G. Sarau, H. Holtmannspötter, M. Pischetsrieder, S.H. Christiansen, W. Dicke, Small-sized microplastics and pigmented particles in bottled mineral water, Water Res. 141 (2018) 307–316. https://doi.org/10.1016/j.watres.2018.05.027.

[18] D. Schymanski, C. Goldbeck, H.U. Humpf, P. Fürst, Analysis of microplastics in water by micro-Raman spectroscopy: Release of plastic particles from different packaging into mineral water, Water Res. 129 (2018) 154–162. https://doi.org/10.1016/j.watres.2017.11.011.

[19] A. Winkler, N. Santo, M.A. Ortenzi, E. Bolzoni, R. Bacchetta, P. Tremolada, Does mechanical stress cause microplastic release from plastic water bottles?, Water Res. 166 (2019) 115082. https://doi.org/10.1016/j.watres.2019.115082.

[20] M. Ferrante, G. Oliveri Conti, P. Zuccarello, Patent method for the extraction and determination of micro- and nano-plastics in organic and inorganic matrix samples: An application on vegetals, MethodsX. 7 (2020) 100989. https://doi.org/10.1016/j.mex.2020.100989.

[21] A.I. Catarino, N. Zhiyue, D.A. M, B. Mattias, M. Julie, V. Michiel, E. Gert, Development of cost-effective methodologies to identify and quantify microplastics in seawater samples, in: Poster Pitch, 2005.

[22] N. Meyers, A.I. Catarino, A.M. Declercq, A. Brenan, L. Devriese, M. Vandegehuchte, B. De Witte, C. Janssen, G. Everaert, Microplastic detection and identification by Nile red staining: Towards a semi-automated, cost- and time-effective technique, Sci. Total Environ. 823 (2022) 153441. https://doi.org/10.1016/j.scitotenv.2022.153441.

[23] L. Lv, J. Qu, Z. Yu, D. Chen, C. Zhou, P. Hong, S. Sun, C. Li, A simple method for detecting and quantifying microplastics utilizing fluorescent dyes - Safranine T, fluorescein isophosphate, Nile red based on thermal expansion and contraction property, Environ. Pollut. 255 (2019) 113283. https://doi.org/10.1016/j.envpol.2019.113283.

[24] S. Konde, J. Ornik, J.A. Prume, J. Taiber, M. Koch, Exploring the potential of photoluminescence spectroscopy in combination with Nile Red staining for microplastic detection, Mar. Pollut. Bull. 159 (2020) 111475. https://doi.org/10.1016/j.marpolbul.2020.111475.

[25] M.T. Sturm, H. Horn, K. Schuhen, The potential of fluorescent dyes — comparative study of Nile red and three derivatives for the detection of microplastics, (2021) 1059–1071.

[26] W.J. Shim, Y.K. Song, S.H. Hong, M. Jang, Identification and quantification of microplastics using Nile Red staining, Mar. Pollut. Bull. 113 (2016) 469–476. https://doi.org/10.1016/j.marpolbul.2016.10.049.

[27] M. Tamminga, Nile Red Staining as a Subsidiary Method for Microplastic Quantification: A Comparison of Three Solvents and Factors Influencing Application Reliability, SDRP J. Earth Sci. Environ. Stud. 2 (2017) 165–172. https://doi.org/10.15436/jeses.2.2.1.

[28] A.I. Catarino, V. Macchia, W.G. Sanderson, R.C. Thompson, T.B. Henry, Low levels of microplastics (MP) in wild mussels indicate that MP ingestion by humans is minimal compared to exposure via household fibres fallout during a meal, Environ. Pollut. 237 (2018) 675–684. https://doi.org/10.1016/j.envpol.2018.02.069.

[29] K.J. Wiggin, E.B. Holland, Validation and application of cost and time effective methods for the detection of 3–500 Mm sized microplastics in the urban marine and estuarine environments surrounding Long Beach, California, Mar. Pollut. Bull. 143 (2019) 152–162. https://doi.org/10.1016/j.marpolbul.2019.03.060.

[30] K. Dowarah, A. Patchaiyappan, C. Thirunavukkarasu, S. Jayakumar, S.P. Devipriya, Quantification of microplastics using Nile Red in two bivalve species Perna viridis and Meretrix meretrix from three estuaries in Pondicherry, India and microplastic uptake by local communities through bivalve diet, Mar. Pollut. Bull. 153 (2020) 110982. https://doi.org/10.1016/j.marpolbul.2020.110982.

[31] J.C. Prata, J.P. da Costa, A.C. Duarte, T. Rocha-Santos, Methods for sampling and detection of microplastics in water and sediment: A critical review, TrAC - Trends Anal. Chem. 110 (2019) 150–159. https://doi.org/10.1016/j.trac.2018.10.029.

[32] J.C. Prata, J.R. Alves, J.P. da Costa, A.C. Duarte, T. Rocha-Santos, Major factors influencing the quantification of Nile Red stained microplastics and improved automatic quantification (MP-VAT 2.0), Sci. Total Environ. 719 (2020) 137498. https://doi.org/10.1016/j.scitotenv.2020.137498.

[33] G. Erni-Cassola, M.I. Gibson, R.C. Thompson, J.A. Christie-Oleza, Lost, but Found with Nile Red: A Novel Method for Detecting and Quantifying Small Microplastics (1 mm to 20 μm) in Environmental Samples, Environ. Sci. Technol. 51 (2017) 13641–13648. https://doi.org/10.1021/acs.est.7b04512.

[34] T. Maes, R. Jessop, N. Wellner, K. Haupt, A.G. Mayes, A rapid-screening approach to detect and quantify microplastics based on fluorescent tagging with Nile Red, Sci. Rep. 7 (2017) 1–10. https://doi.org/10.1038/srep44501.

[35] J.C. Prata, V. Reis, J.T.V. Matos, J.P. da Costa, A.C. Duarte, T. Rocha-Santos, A new approach for routine quantification of microplastics using Nile Red and automated software (MP-VAT), Sci. Total Environ. 690 (2019) 1277–1283. https://doi.org/10.1016/j.scitotenv.2019.07.060.

[36] L.B. Ayres, F.J.V. Gomez, J.R. Linton, M.F. Silva, C.D. Garcia, Taking the leap between analytical chemistry and artificial intelligence: A tutorial review, Anal. Chim. Acta. 1161 (2021) 338403. https://doi.org/10.1016/j.aca.2021.338403.

[37] S. Berg, D. Kutra, T. Kroeger, C.N. Straehle, B.X. Kausler, C. Haubold, M. Schiegg, J. Ales, T. Beier, M. Rudy, K. Eren, J.I. Cervantes, B. Xu, F. Beuttenmueller, A. Wolny, C. Zhang, U. Koethe, F.A. Hamprecht, A. Kreshuk, Ilastik: Interactive Machine Learning for (Bio)Image Analysis, Nat. Methods. 16 (2019) 1226–1232. https://doi.org/10.1038/s41592-019-0582-9.

[38] C.H. Li, P.K.S. Tam, An iterative algorithm for minimum cross entropy thresholding, Pattern Recognit. Lett. 19 (1998) 771–776. https://doi.org/10.1016/S0167-8655(98)00057-9.

[39] I. V Kirstein, F. Hensel, A. Gomiero, L. Iordachescu, A. Vianello, H.B. Wittgren, J. Vollertsen, Drinking plastics? – Quantification and qualification of microplastics in drinking water distribution systems by μFTIR and Py-GCMS, Water Res. 188 (2021) 116519. https://doi.org/10.1016/j.watres.2020.116519.

[40] P.S. Bäuerlein, M.W. Erich, W.M.G.M. van Loon, S.M. Mintenig, A.A. Koelmans, A monitoring and data analysis method for microplastics in marine sediments, Mar. Environ. Res. 183 (2023) 105804. https://doi.org/10.1016/j.marenvres.2022.105804.

[41] M. Simon, N. van Alst, J. Vollertsen, Quantification of microplastic mass and removal rates at wastewater treatment plants applying Focal Plane Array (FPA)-based Fourier Transform Infrared (FT-IR) imaging, Water Res. 142 (2018) 1–9. https://doi.org/10.1016/j.watres.2018.05.019.

[42] AOAC_International, AOAC Guidelines for Single Laboratory Validation of Chemical Methods for Dietary Supplements and Botanicals, Arlington, 2002.

[43] A.P. Jost, J.C. Waters, Designing a rigorous microscopy experiment: Validating methods and avoiding bias, J. Cell Biol. 218 (2019) 1452–1466. https://doi.org/10.1083/jcb.201812109.

[44] S. Taheri, B. Shoshtari-Yeganeh, H. Pourzamani, K. Ebrahimpour, Investigating the pollution of bottled water by the microplastics (MPs): the effects of mechanical stress, sunlight exposure, and freezing on MPs release, Environ. Monit. Assess. 195 (2023). https://doi.org/10.1007/s10661-022-10697-2.

[45] S.M. Praveena, N.I. Shamsul Ariffin, A.L. Nafisyah, Microplastics in Malaysian bottled water brands: Occurrence and potential human exposure, Environ. Pollut. 315 (2022) 120494. https://doi.org/10.1016/j.envpol.2022.120494.

[46] M. Ravanbakhsh, M. Ravanbakhsh, H.A. Jamali, M. Ranjbaran, S. Shahsavari, N. Jaafarzadeh Haghighi Fard, The effects of storage time and sunlight on microplastic pollution in bottled mineral water, Water Environ. J. (2022) 1–12. https://doi.org/10.1111/wej.12829.

[47] S. Samandra, O.J. Mescall, K. Plaisted, B. Symons, S. Xie, A. V. Ellis, B.O. Clarke, Assessing exposure of the Australian

population to microplastics through bottled water consumption, Sci. Total Environ. 837 (2022) 155329. https://doi.org/10.1016/j.scitotenv.2022.155329.

[48] C.N. Ibeto, C.E. Enyoh, A.C. Ofomatah, L.A. Oguejiofor, T. Okafocha, V. Okanya, Microplastics pollution indices of bottled water from South Eastern Nigeria, Int. J. Environ. Anal. Chem. 00 (2021) 1–20. https://doi.org/10.1080/03067319.2021.1982926.

[49] A. Altunışık, Microplastic pollution and human risk assessment in Turkish bottled natural and mineral waters, Environ. Sci. Pollut. Res. (2023). https://doi.org/10.1007/s11356-022-25054-6.

[50] M.M.-L. Leung, Y.-W. Ho, C.-H. Lee, Y. Wang, M. Hu, K.W.-H. Kwok, S.-L. Chua, J.K.-H. Fang, Improved Raman spectroscopy-based approach to assess microplastics in seafood, Environ. Pollut. 289 (2021) 117648. https://doi.org/10.1016/J.ENVPOL.2021.117648.

[51] H. LI, L. ZHU, M. MA, H. WU, L. AN, Z. YANG, Occurrence of microplastics in commercially sold bottled water, Sci. Total Environ. 867 (2023) 161553. https://doi.org/10.1016/j.scitotenv.2023.161553.

[52] J. Nizamali, S.M. Mintenig, A.A. Koelmans, Assessing microplastic characteristics in bottled drinking water and air deposition samples using laser direct infrared imaging, J. Hazard. Mater. 441 (2023) 129942. https://doi.org/10.1016/j.jhazmat.2022.129942.

[53] Y. Tse, S.M. Chan, E.T. Sze, Quantitative Assessment of Full Size Microplastics in Bottled and Tap Water Samples in Hong Kong, (2022).

[54] P. Zuccarello, M. Ferrante, A. Cristaldi, C. Copat, A. Grasso, D. Sangregorio, M. Fiore, G. Oliveri Conti, Exposure to microplastics (<10 Mm) associated to plastic bottles mineral water consumption: The first quantitative study, Water Res. 157 (2019) 365–371. https://doi.org/10.1016/j.watres.2019.03.091.

[55] G. Oliveri Conti, M. Ferrante, M. Banni, C. Favara, I. Nicolosi, A. Cristaldi, M. Fiore, P. Zuccarello, Micro- and nano-plastics in edible fruit and vegetables. The first diet risks assessment for the general population, Environ. Res. 187 (2020) 109677. https://doi.org/10.1016/j.envres.2020.109677.

[56] E. Lee, S. Lee, Y. Chang, Lee, Simple screening of microplastics in bottled waters and environmental freshwaters using a novel fluorophore, Chemosphere. 285 (2021) 131406. https://doi.org/10.1016/j.chemosphere.2021.131406.

Figure legend

Graphical abstract *[Print in color]*

Figure 1 → Workflow for the analysis of microplastics in bottled water by Nile Red staining and fluorescence microscopy. The sample (A) is preconcentrated and stained in the filtration unit. After an incubation of 15 min, the filtration is completed (B). Images are acquired under the fluorescence microscope (C). The automated image processing (D) yields both qualitative as well as quantitative data of the stained particles (E). *[Print in color]*

Figure 2 → Preliminary evaluation of the Random Forest classifier developed in Ilastik for the segmentation of fluorescence microscopy images of Nile Red stained microplastics (MPs). Test set (left column) and corresponding binarized masks (right column) produced by the final Random Forest model, included in the Ilastik-based workflow. The test set included: (A) an image lacking fluorescent particles obtained from the analysis of a blank sample of ultra-pure water; (B) an image of Nile Red stained standard polyethylene (PE) MPs obtained from the analysis of a spiked sample of ultra-pure water; (C) a crowded image of Nile Red stained standard PE obtained from the analysis of a spiked sample of ultra-pure water; (D) and (E) images of Nile Red stained particles isolated from real samples of commercial bottled water. *[Print in color]*

Figure 3 → Comparison of polycarbonate, alumina, and cellulose nitrate filters for their suitability for the analysis of microplastics (MPs) by Nile Red staining and fluorescence microscopy. A recovery study was performed on ultrapure-water samples spiked with polyethylene (PE) MPs at the concentration level of 0.1 ppm and 1 ppm. MPs in suspension were stained with Nile Red, then equal aliquots of the suspension were filtrated with filters of the three different materials. The isolated MPs were analyzed via the fluorescence microscopy and ImageJ image analysis method. Sample images of Nile Red stained PE MPs isolated on (A) black polycarbonate membrane filter, (B) alumina filter membrane, and (C) cellulose nitrate filter. (D) Computed recovery from image analysis of PE MPs isolated and analyzed on filters of the three different materials; average ± SD (n = 3). *[Print in color]*

Figure 4 → Method performance characteristics. (A) Evaluation of the accuracy and precision in particle size measurements. Vertical error bars refer to standard deviation (SD) for n = 5 individual particles, horizontal error bars refer to SD of particle size as reported in the size certificate of the analytical standard. (B) Study of linearity and working range in microplastics quantification. Error bars represent 95% confidence interval (C.I.). (C) Repeatability and within-lab reproducibility for microplastic quantification. (D) Recovery study. *[b/w figure]*

Figure 5 → Microplastics analysis in real samples. (A) Number of Nile Red stained microparticle in 500 mL of bottled water. Boxplots of bootstrap estimates, see text. Each box illustrates first quartile, second quartile, and median of the estimated distributions, whiskers represent 95% confidence intervals (C.I.). LOQ, Limit of Quantification; mLOD, method Limit of Detection. (B) Size distribution of the analyzed Nile Red stained microparticles. DL, detection limit as per particle size; IQR, interquartile range. *[Print in color]*

Graphical abstract

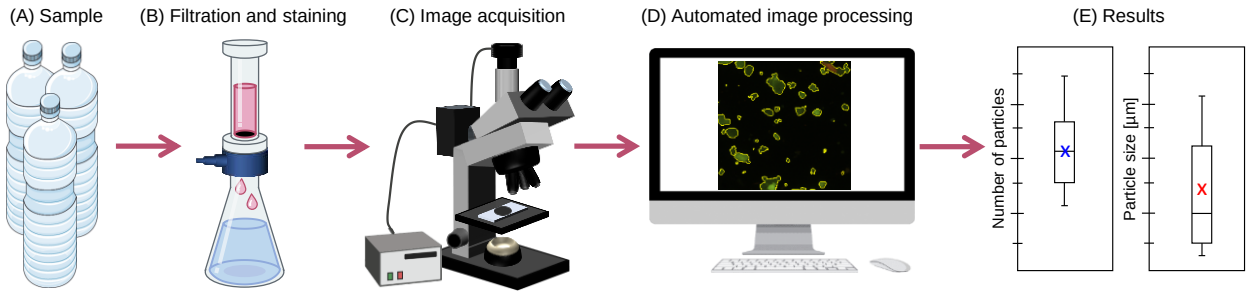

Figure 1. *Workflow for the analysis of microplastics in bottled water by Nile Red staining and fluorescence microscopy. The sample (A) is preconcentrated and stained in the filtration unit. After an incubation of 15 min, the filtration is completed (B). Images are acquired under the fluorescence microscope (C). The automated image processing (D) yields both qualitative as well as quantitative data of the stained particles (E).*

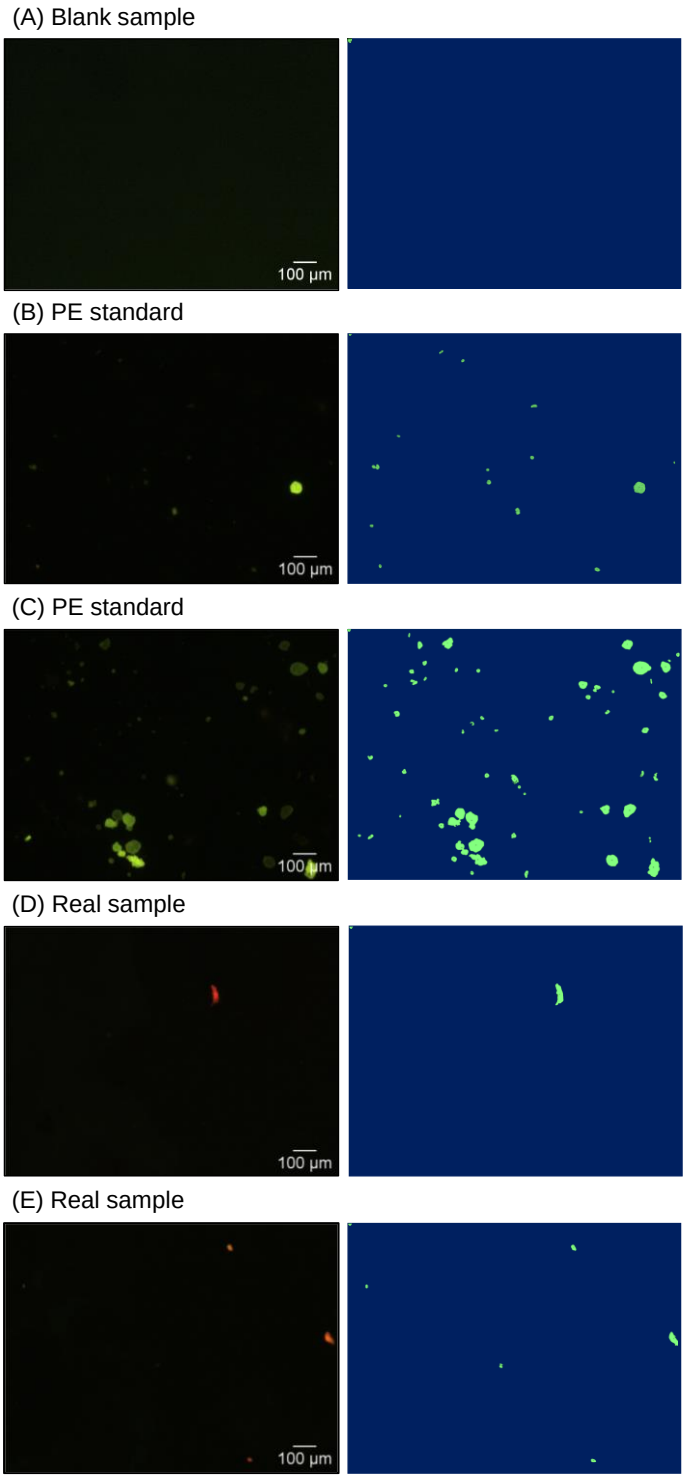

Figure 2. *Preliminary evaluation of the Random Forest classifier developed in Ilastik for the segmentation of fluorescence microscopy images of Nile Red stained microplastics (MPs). Test set (left column) and corresponding binarized masks (right column) produced by the final Random Forest model, included in the Ilastik-based workflow. The test set included: (A) an image lacking fluorescent particles obtained from the analysis of a blank sample of ultra-pure water; (B) an image of Nile Red stained standard*

polyethylene (PE) MPs obtained from the analysis of a spiked sample of ultra-pure water; (C) a crowded image of Nile Red stained standard PE obtained from the analysis of a spiked sample of ultra-pure water; (D) and (E) images of Nile Red stained particles isolated from real samples of commercial bottled water.

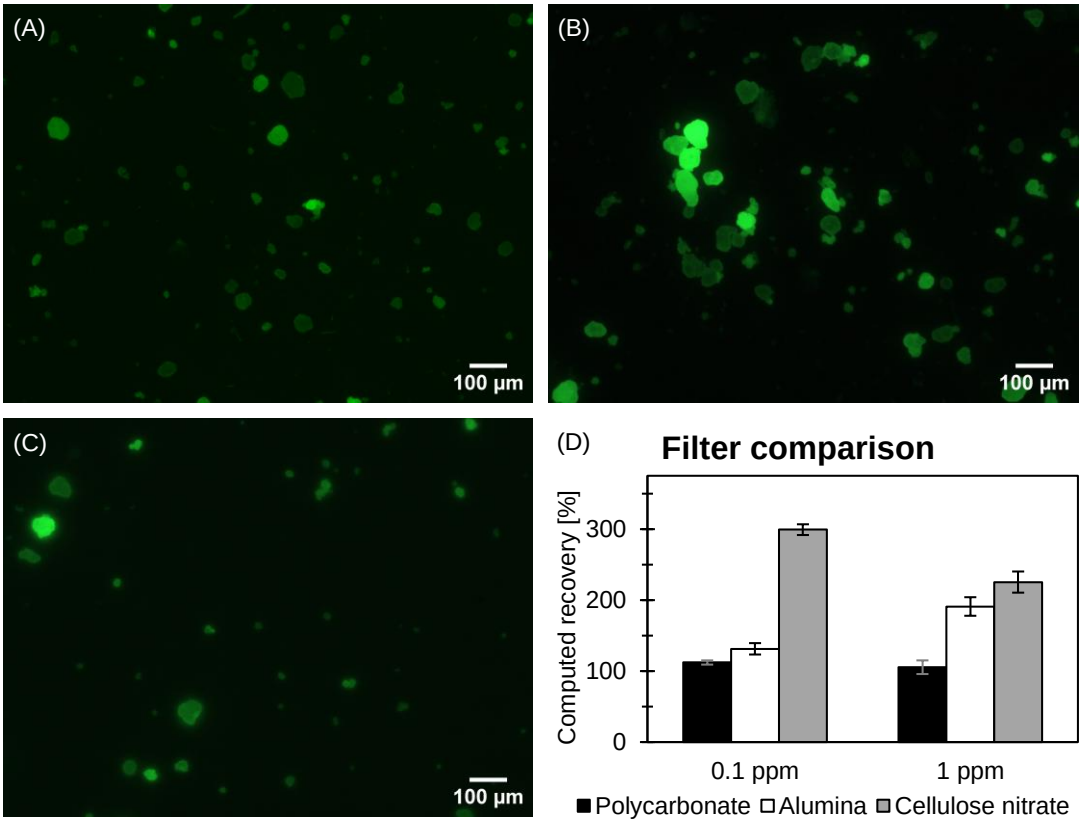

Figure 3. *Comparison of polycarbonate, alumina, and cellulose nitrate filters for their suitability for the analysis of microplastics (MPs) by Nile Red staining and fluorescence microscopy. A recovery study was performed on ultrapure-water samples spiked with polyethylene (PE) MPs at the concentration level of 0.1 ppm and 1 ppm. MPs in suspension were stained with Nile Red, then equal aliquots of the suspension were filtrated with filters of the three different materials. The isolated MPs were analyzed via the fluorescence microscopy and ImageJ image analysis method. Sample images of Nile Red stained PE MPs isolated on (A) black polycarbonate membrane filter, (B) alumina filter membrane, and (C) cellulose nitrate filter. (D) Computed recovery from image analysis of PE MPs isolated and analyzed on filters of the three different materials; average ± SD (n = 3).*

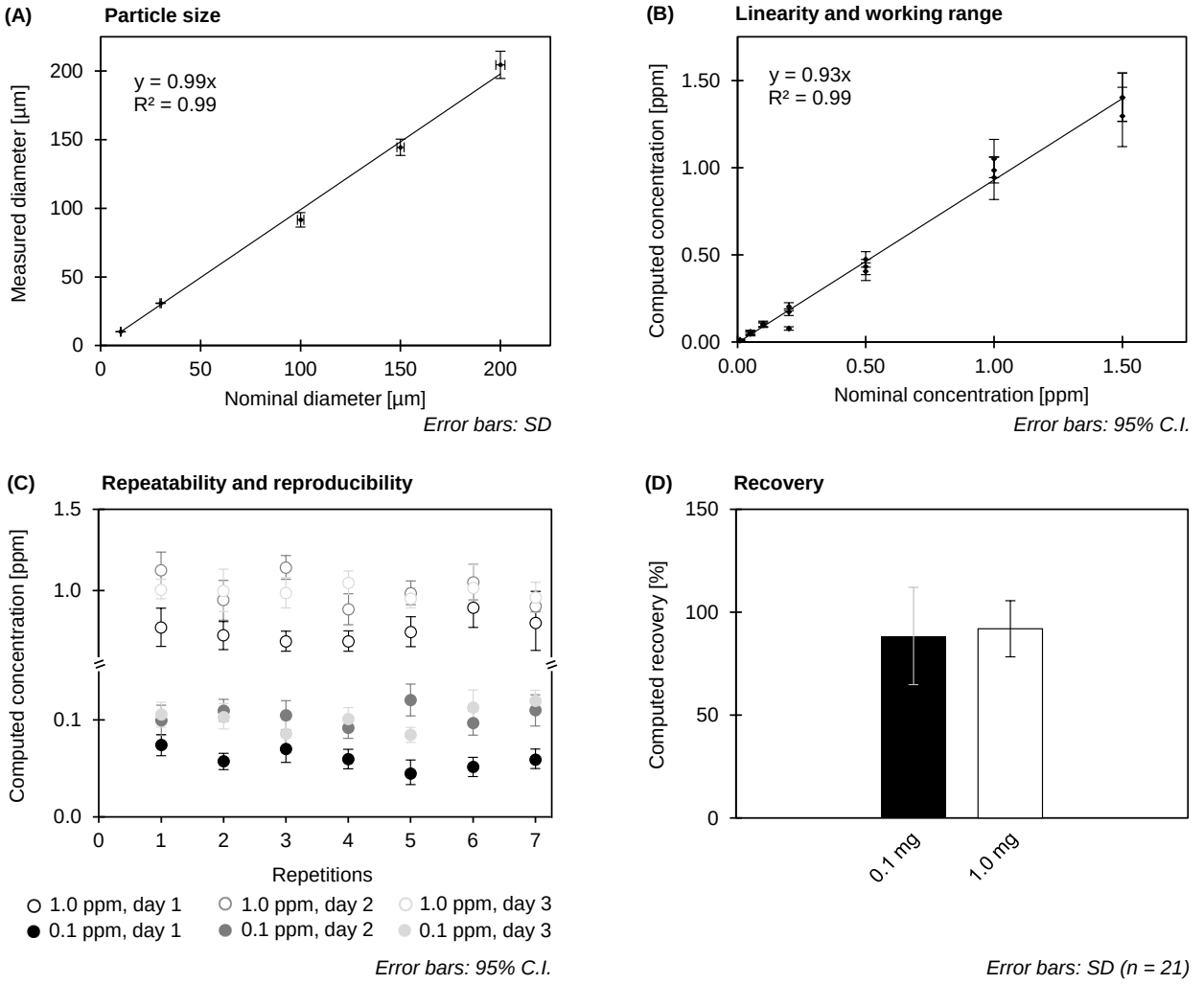

Figure 4. *Method performance characteristics. (A) Evaluation of the accuracy and precision in particle size measurements. Vertical error bars refer to standard deviation (SD) for n = 5 individual particles, horizontal error bars refer to SD of particle size as reported in the size certificate of the analytical standard. (B) Study of linearity and working range in microplastics quantification. Error bars represent 95% confidence interval (C.I.). (C) Repeatability and within-lab reproducibility for microplastic quantification. (D) Recovery study.*

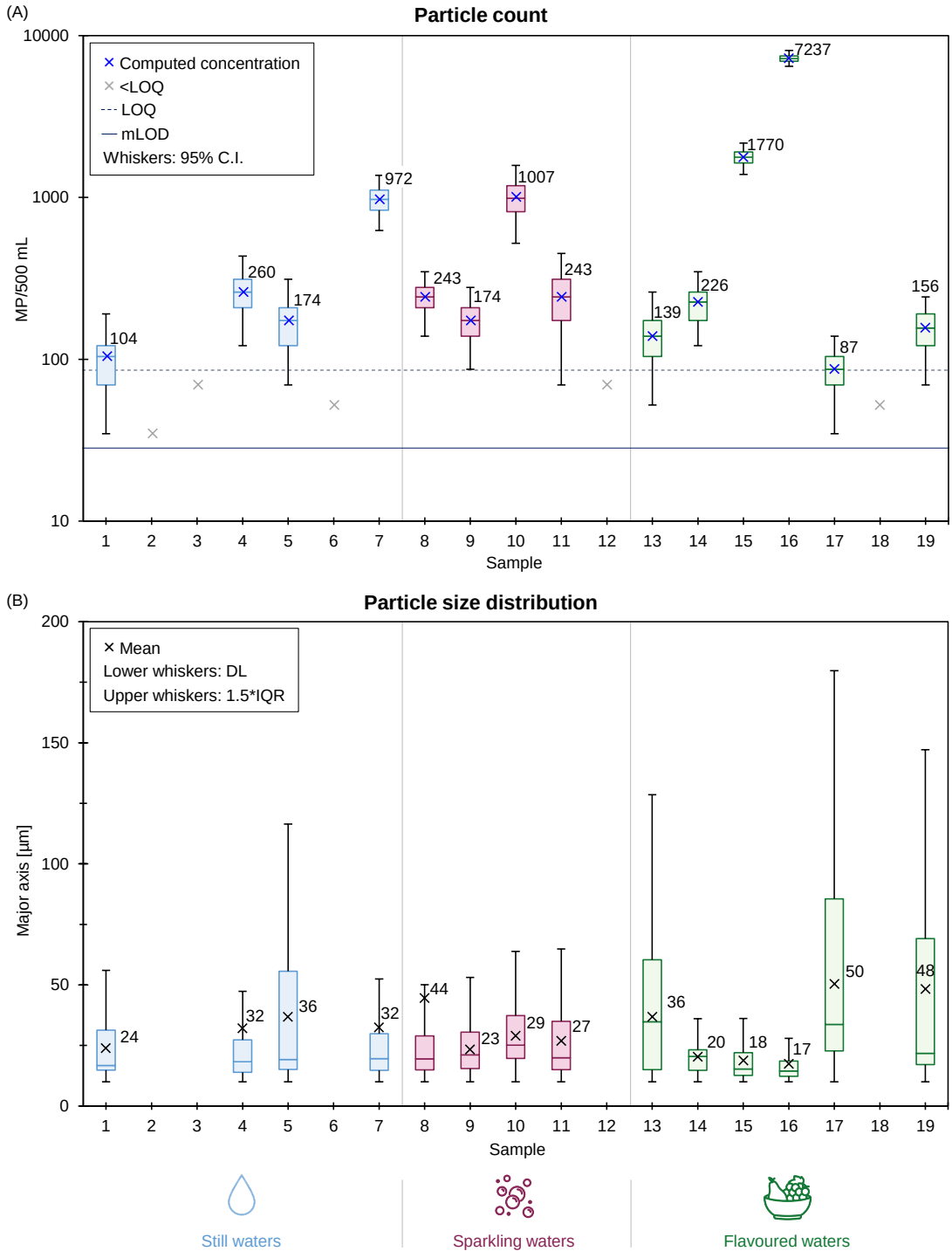

Figure 5. *Microplastics analysis in real samples. (A) Number of Nile Red stained microparticle in 500 mL of bottled water. Boxplots of bootstrap estimates, see text. Each box illustrates first quartile, second quartile, and median of the estimated distributions, whiskers represent 95% confidence intervals (C.I.). LOQ, Limit of Quantification; mLOD, method Limit of Detection. (B) Size distribution of the analyzed Nile Red stained microparticles. DL, detection limit as per particle size; IQR, interquartile range.*

Table legend

Table 1 → Reported level of microplastic contamination in bottled water

Table 1. Reported level of microplastic contamination in bottled water

Sample	Sample number	MP count min – max (Mean ± SD)	Size range [µm]	Reference
Still bottled water	7	<LOQ - 972 (95% CI [625, 1372])[a]	10 - 310	This study
Sparkling bottled water	5	<LOQ - 1007 (95% CI [521, 1579])[a]		
Flavored bottled water	8	ND - 7237 (95% CI [6456, 8088])[a]		
Natural bottled water	105	2 - 20[b] (4.6 ± 3.9)[b]	6 - 1000	Altunışık *et al*., 2023 [49]
Mineral bottled water	45	5 - 35[b] (12.6 ± 8.7)[b]		
Bottled water	100	0.3 ± 0.6 - 6.7 ± 5.51[b] (2.2 ± 1.9)[c]	> 11	Ibeto *et al*., 2021 [48]
Bottled water	65	(140 ± 19)[b]	> 6.5	Kankanige *et al*., 2020 [14]
Bottled water	3	(3.6)[b]	100 - 5 000	Kosuth *et al*., 2018 [10]
Mineral bottled water	4	12 - 58[b]	40 - 723	Lee *et al*., 2021 [56]
Sparkling bottled water	4	6 - 22[b]		
Bottled water	7	(65.6 ± 44.7)[b]	10 - 500	Li *et al*., 2022 [51]
Bottled water	11	0 - 36[b] (8.5 ± 10.2)[b]	1 280 - 4 200	Makhdoumi *et al*., 2021 [11]
Bottled water	259	0 - 10 390[b] (325)[b]	> 6.5	Mason *et al*., 2018 [12]
Bottled water	9	4 - 216[b] (57 ± 76)[b]	10 - 5 000	Nizamali *et al*., 2023 [52]
Bottled water	10	(2 649 ± 2 857)[b]	> 1	Oßmann *et al*., 2018 [17]
Bottled water	8	8 - 22[b] (11.7 ± 4.6)[b]	25 - 5 000	Praveena *et al*.2022 [45]
Bottled water	27	(41.1 ± 9.0)[b]	<1 000	Ravanbakhsh *et al*., 2022 [46]
Bottled water	48	0 - 80[b] (13 ± 19)[b]	6 - 480	Samandra *et al*., 2022 [47]
Bottled water	11	2 - 44[b] (14 ± 14)[b]	1 - 500	Schymanski *et al*., 2018 [18]
Bottled water	23	199.8 - 6 626.7[b] (1 496.7 ± 1 452.2)[b]	1 - 47	Taheri *et al*., 2023 [44]
Bottled water	9	(8 955 ± 5 205)[b]	1 - 5 000	Tse *et al*., 2022 [53]
Bottled water	18	ND	1 - 40	Winkler *et al*., 2019 [19]
Bottled water	69	2 - 23[d]	25 - 5 000	Zhou *et al*., 2021 [16]
Bottled water	30	3.16E+07 - 1.1E+08[b] (5.42E+07 ± 1.95E+07)[b]	1.3 - 4.2	Zuccarello *et al*., 2019 [54]

[a] items/0.5L; [b] items/L; [c] items/0.75L; [d] items/bottle. CI, Confidence Interval; LOQ, Limit of Quantification; MP, microplastics; ND, Not Detected; SD, Standard Deviation.